JPE 17-5-25

https://doi.org/10.6113/JPE.2017.17.5.1382
ISSN(Print): 1598-2092 / ISSN(Online): 2093-4718

Isolated Power Supply for Multiple Gate Drivers using Wireless Power Transfer System with Single-Antenna Receiver

Chang-Jong Lim* and Shihong Park†

*,†Dept. of Electrical and Electronic Eng., Dankook University, Yongin, Korea

Abstract

This paper presents a power supply for gate drivers, which uses a magnetic resonance wireless power transfer system. Unlike other methods where multiple antennas are used to supply power for the gate drivers, the proposed method uses a single antenna in an insulated receiver to make multiple mutually isolated power supplies. The power transmitted via single antenna is distributed to multiple power supplies for gate drivers through resonant capacitors connected in parallel that also block DC bias. This approach has many advantages over other methods, where each gate driver needs to be supplied with power using multiple receiver antennas. The proposed method will therefore lead to a reduction in production costs and circuit area. Because the proposed circuit uses a high resonance frequency of 6.78 MHz, it is possible to implement a transmitter and a receiver using a small-sized spiral printed-circuit-board-type antenna. This paper used a single phase-leg circuit configuration to experimentally verify the performance characteristics of the proposed method.

Key words: Galvanic isolation, Isolated power supply, Multiple gate drive, Transformerless, Wireless power transfer

I. INTRODUCTION

In the phase-leg configuration using power MOSFET switches, a gate-driver power supply is required to operate the switches [1]. For the high-side switch, an N-type switch is widely used because it has better switching characteristics and smaller on-resistances than a P-type switch; therefore, a separate floating power supply is necessary. Fig. 1 shows the conventional single phase-leg configuration that uses a floating power supply, and the level-shift circuit for operating the high-side N-type switch. The power supply for the high-side switches in a low-power application normally uses a bootstrap method or an improved charge-pump method [2], [3]. However, in higher voltage and power applications, a galvanic-isolation technique is used to protect the gate signals and the power supply from the noise generated during switching. Generally, a transformer is widely used to provide isolated power supply for galvanic isolation. This method, however, increases the cost and circuit area, as it requires customized coils. To overcome the disadvantages as shown in Fig. 2, recent studies proposed designing an isolated power supply using a wireless power transfer system [4]-[7]. The isolated power supply using the magnetic resonance method has high Q(Quality factor), which allows long-distance transmission. Therefore, this approach is suitable for the galvanic isolation of the power supply. Also, it can make a transmitter (Tx) system using a single antenna, which in turn can make receiver (Rx) systems in multiple gate drivers. This approach will indeed reduce the cost and circuit area, but will face constraints as it will have to use multiple receiver antennas. Therefore, this paper proposes a new isolated power supply design with a magnetic resonance wireless power transfer system to supply isolated power to multiple gate drivers using a single Tx and Rx antenna.

This paper consists of five sections including the introduction. In Section II, a mathematical model of the magnetic resonance wireless power transfer system is proposed. The proposed system is described in detail in Section III. In Section IV, the circuit design, the test board manufactured based on the proposed method, and the measured results are presented. Finally, in Section V, the conclusions are summarized.

Manuscript received Jan. 31, 2017; accepted May 21, 2017
Recommended for publication by Associate Editor Yijie Wang.
†Corresponding Author: Shihongpark@gmail.com
Tel: +82-031-8005-3629, Dankook University
*Dept. of Electronic and Electrical Eng., Dankook University, Korea

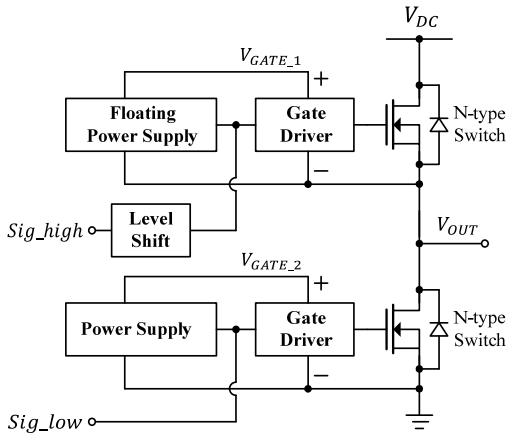

Fig. 1. Conventional phase-leg configuration.

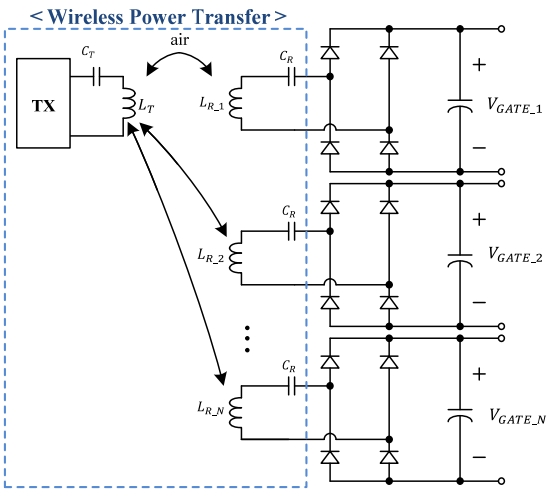

Fig. 2. Conventional wireless isolated power supply for multiple gate driver.

II. Mathematical Model for Magnetic Resonance Wireless Power Transfer

Fig. 3 shows a diagram that describes the principle of wireless power transfer using magnetic resonance. The power is transmitted at the resonance frequency of the LC circuits of the Tx and Rx antennas. Since the transmission frequency of Tx is fixed, the transmission gain can be controlled by varying the resonance frequencies of the Tx and Rx antennas [8].

The resonance frequency is defined as follows:

$$f_{resonance} = \frac{1}{2\pi\sqrt{L_R C_R}} \tag{1}$$

In order to understand the operation of the magnetic resonance coupled circuit, one should first study the coupled-circuit model and the reflected impedance concept [9], [10]. The diagram of a magnetic resonance circuit model is shown in Fig. 4. C_1, C_2, and L_2 represent the L-C resonance tanks of the Tx and Rx, R_1 and R_2 represent the parasitic resistances in the antennas, and R_L represents the load.

To calculate the impedance looking into the input, the load is shorted, and the reflected impedance is calculated as follow.

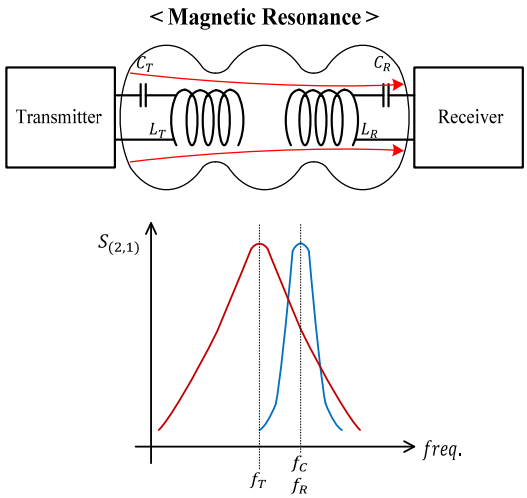

f_T = transmitter resonance frequency
f_R = receiver resonance frequency
f_C = carrier frequency

Fig. 3. Magnetic resonance wireless power transfer model.

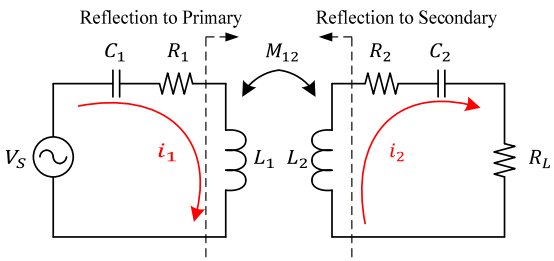

Fig. 4. Magnetic resonance wireless power transfer model.

According to Kirchhoff's voltage law, the primary side can be represented as:

$$Z_1 = R_1 + jwL_1 + \frac{1}{jwC_1} \tag{2}$$

$$Z_2 = R_2 + jwL_2 + \frac{1}{jwC_2} \tag{3}$$

$$Z_M = jwM_{12} = jwM_{21} = jwM \tag{4}$$

$$V_S = I_1 Z_1 - I_2 Z_M \tag{5}$$

and the secondary side as:

$$0 = -I_1 Z_M + I_2 Z_2 \tag{6}$$

$$I_2 = \frac{I_1 Z_M}{Z_2} \tag{7}$$

The input impedance is then calculated by substituting (7) into (5) as follows:

$$Z_{eq} = \frac{V_S}{I_1} = Z_1 - \frac{Z_M{}^2}{Z_2} = Z_1 - \frac{w^2 M^2}{Z_2} \tag{8}$$

Then, the reflected impedance is:

$$Z_{reflected} = \frac{w^2 M^2}{Z_2} \tag{9}$$

Fig. 5 shows a magnetic resonance coupled model that reflects the mathematical configurations above. It shows that the current on the secondary side and the reflected voltage ($jwMi_1$) can be controlled by adjusting the current on the primary side [11].

Fig. 6 shows the wireless power transfer model and output voltage for the isolated power supply presented in this paper.

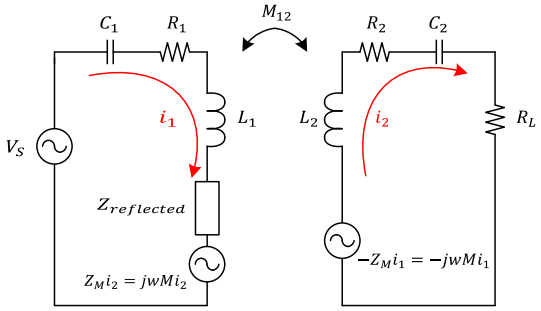

Fig. 5. Magnetic resonance coupled circuit model.

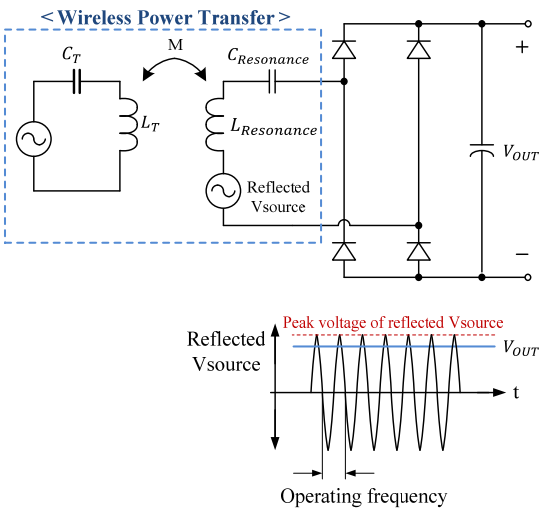

Fig. 6. Wireless power transfer model and waveforms of output voltage.

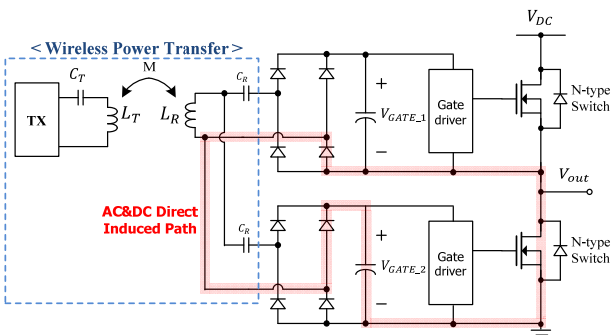

Fig. 7. Seemingly possible idea for multiple outputs with single antenna for a phase leg configuration.

The primary side can be described as a Tx system, and the secondary side can be described as a Rx system. Thus, as mentioned above, the voltage transmitted to the Rx can be modeled as current controlled voltage source controlled by the Tx. It also shows that the maximum output voltage is limited by Tx system. The maximum output voltage in Rx can be obtained under no-load conditions. Therefore it is apparent that the maximum output voltage is equal to the reflected voltage ($jwMi_1$), since there is no voltage drop in R, L and C due to zero current conditions in Rx.

$$V_{OUT} = jwMi_1 \ (at\ no\ load\ condition) \quad (10)$$

III. Simple Configuration Method Using A Single Receiving Antenna

This paper proposes a method to supply isolated power supply to multiple gate drivers using only a single Rx antenna in the wireless power transfer system, by providing an output path in parallel with the coil (L_R) used in the Rx antenna. Fig. 7 shows one seemingly possible idea to provide multiple output voltages using one Rx antenna [12], [13]. To maintain the resonance frequency of the circuit connected in parallel, the resonance capacitor is selected as follows.

$$C_R = \frac{C_{Resonance}}{2} \quad (11)$$

$$f_{resonance} = \frac{1}{2\pi\sqrt{L_R C_R}} \quad (12)$$

The two output voltage V_{GATE_1} and V_{GATE_2} are used as power supply for the gate driver circuit to drive each N-type switch in a single phase-leg circuit as shown in Fig. 7. However, in this case, the highlighted current path is generated from one power supply to another when the high-side switch turns on. This condition results in the destruction of low-side gate drive and switch due to high voltage stress. Therefore, isolation between each of the power supplies is crucial when only a single Rx antenna is used for multiple gate drivers.

In this paper, the resonance capacitor in the Rx resonant tank circuit is distributed to the rectifier at each power supply in order to block the DC path and minimize the interference from other power supplies during switching. Fig. 8 shows the proposed circuit. The value of the distributed capacitor (C_{R_DIS}) required to maintain the resonance frequency of the Rx system can be calculated as follows.

$$C_{R\_DIS} = \frac{2C_{Resonance}}{N} \quad (13)$$

$$C_{R\_DIS,Total} = \sum_1^N \frac{2C_{Resonance}}{n} \quad (14)$$

$$f_{resonance} = \frac{1}{2\pi\sqrt{L_R C_{R,Total}}} \quad (15)$$

The capacitor (C_{R_DIS}) in the resonant tank blocks the DC voltage to prevent interference from other power supplies.

In the case of AC voltage, the voltage fluctuations from other power supplies appear in the form of ripples, the magnitude of the ripple is determined by the ration of the capacitor in the resonance tank (C_{R_DIS}) to the capacitor in each power supply (C_{VOUT}). When C_{R_DIS} is much smaller than C_{VOUT} ($C_{R\_DIS} << C_{VOUT}$), the ripple magnitude is very small. Therefore, the transient fluctuations in the output voltage during switching can be analyzed in the same manner as the AC voltage conditions. In other words, the current generated by the fluctuations in the output voltage, $\frac{C_{R\_DIS}}{2} \times \frac{d(V_{DC}-V_{GATE\_2})}{dt}$, will have a very small magnitude under the condition $C_{R\_DIS} \ll C_{VOUT}$. Therefore, the distributed capacitor (C_{R_DIS}) effectively blocks the interference resulting from the changes in the output voltages of the different power supplies; thus, it effectively isolates the power supplies. Since the required capacitance of C_{R_DIS} is only a few hundred pF, a compact and low-cost system can be designed even for the

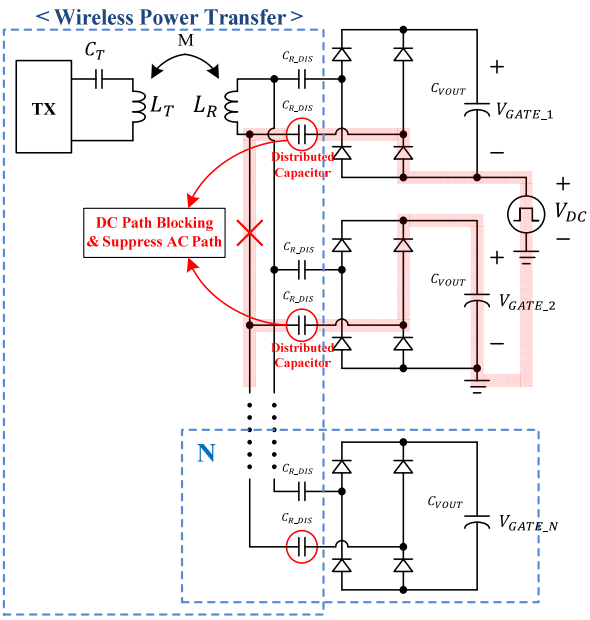

Fig. 8. Seemingly possible idea for multiple outputs with single antenna for a phase leg configuration.

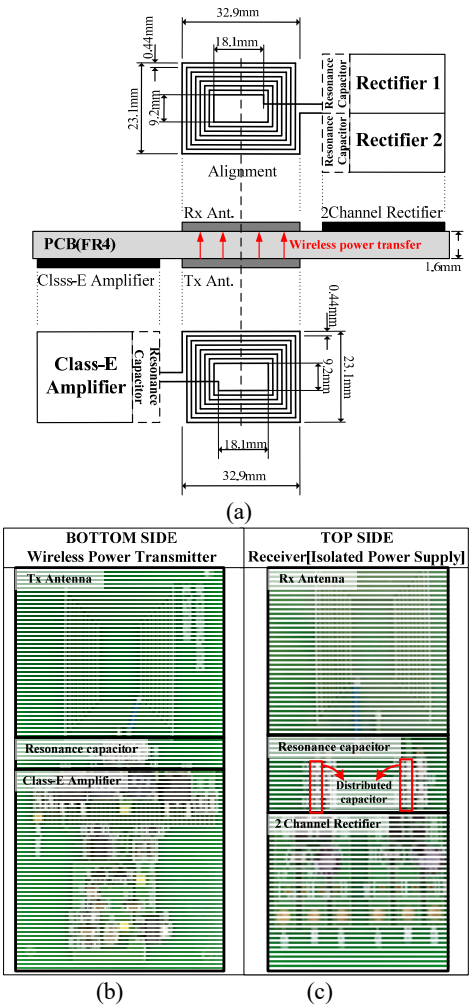

Fig. 9. Design of wireless isolated power supply for multiple gate driver system. (a) Conceptual diagram of test board. (b) Photo of bottom of PCB board featuring Tx. (c) Photo of top of PCB board featuring Rx.

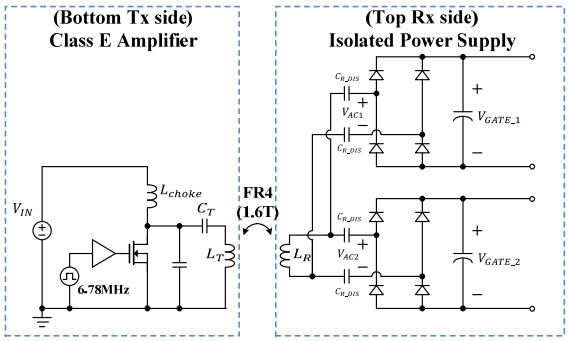

Fig. 10. Design of proposed wireless isolated power supply.

high-voltage applications. The price of 560pF ceramic capacitor with 2.5kV isolation voltage is less than 10 cents in DIGIKEY which is one of the largest online electronic parts shop. However, the cost of ceramic capacitor above 3kV isolation voltage is much higher. In general, the minimum required isolation voltage of the capacitor C_{R_DIS} is 2.5kV under 300V DC link voltage condition for the long-term reliability in high-voltage applications.

IV. Design and Measurement Results

A. Design of Wireless Isolated Power Supply

Fig. 9 shows the test board used to verify the performance characteristics of a proposed wireless isolated power supply system. Fig. 9(a) shows the conceptual diagram of PCB board composed of Tx and Rx. The PCB is composed of 2 layers, and the bottom side is used as Tx and the top side used as Rx. The isolated power supply is transmitted from bottom side Tx to top side Rx. Therefore, it is easy to align Tx and the Rx antenna for better wireless power transmission. The thickness of the PCB used in this design is 1.6mm, and the thickness of the copper foil used as the antenna was designed to be 2 oz. Fig. 9(a) shows the cross-sectional diagram and top views of the Tx and Rx antennas. Because wireless power transfer is done using a high resonance frequency of 6.78 MHz [14], it was possible to implement antennas of small sizes. The shape of the antenna is a spiral printed-circuit-board-type inductor and the area of the antenna is $27.56mm^2 (W = 32.9mm, L = 23.1mm)$ Fig. 9(b) and (c) show the photos of the actual Tx board and Rx board designed on the top and bottom sides of the PCB.

Fig. 10 shows the circuit design for the test boards shown in Fig. 9. The Rx system consists of an Rx antenna and two power supplies to make a single phase-leg and provide the isolated power supply. Furthermore, a full-bridge rectifier is used to convert the AC voltage to DC voltage.

B. Test Board of Wireless Isolated Power Supply and Measurement Results

Fig. 11 shows the test circuit of the proposed wireless isolated power supply system and the test conditions are described in Table I. The load resistor, R_{LOAD}, is assigned a 1kΩ resistance value to model the required power for gate

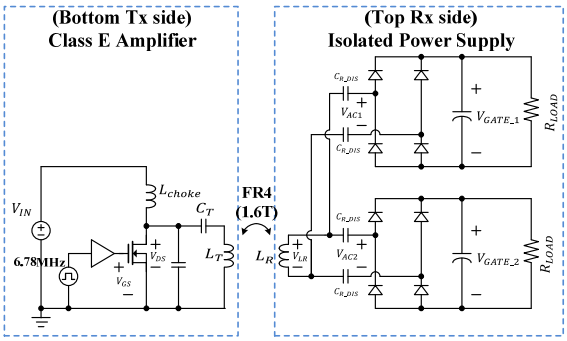

Fig. 11. Test circuit of proposed wireless isolated power supply system.

TABLE I
WIRELESS ISOLATED POWER SUPPLY TEST CONDITIONS

V_{IN}	8 V
Resonance Frequency	6.78 MHz
L_T, L_R	1.8 μH
C_T	1.1 nF
$C_{R\ DIS}$	340 pF
C_{GATE_1}, C_{GATE_2}	10 μF
R_{LOAD}	1 kΩ

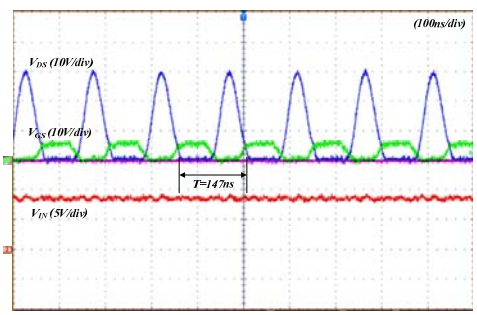

Fig. 12. Waveforms of V_{IN} , V_{DS} and V_{GS} at the transmitter.

drive. This means that the isolated power supply can drive continuous 20mA current or 0.4W power to each gate driver.

The magnitude of V_{IN} is determined by the experiment where V_{GATE} is sufficiently charged up to 20V with 1kΩ load resistor. Therefore, under no-load condition, V_{GATE} is limited 20V by Zener diode in order to protect power switches from over voltage condition. Since V_{GATE} is proportional to the magnitude of V_{IN}, if the higher power is required in each gate driver the higher V_{IN} is needed. However, once the gate charge of power device and its switching frequency is determined, the maximum gate driver power can be calculated. Therefore, in real applications, there is no need to adjust V_{IN}. This is exactly the same concept as the conventional isolated power supply using a transformer. However the selection of an input voltage with a transformer is more flexible because its efficiency is high and turns of coils can be easily altered.

Fig. 12 shows test results of Class-E amplifier. The red line represents V_{IN}, the blue line represents V_{DS}, and the green line represents V_{GS}. The operating frequency is 6.78MHz and voltage of V_{DS} is about 30V. These waveforms demonstrate

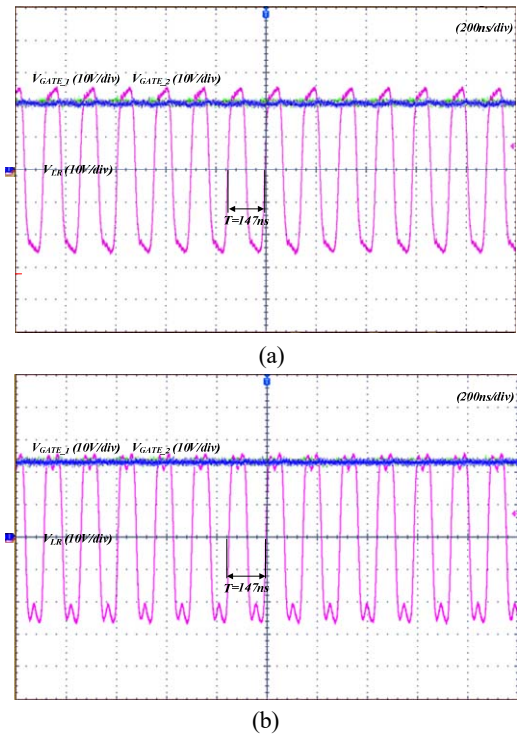

Fig. 13. Waveforms of received output voltage at the receiver. (a) Waveforms of no-load conditions, (b) Waveforms of 1kΩ load conditions.

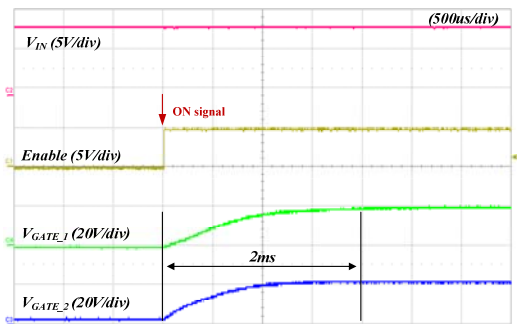

Fig. 14. Waveforms of start-up voltage.

that the class-E Amplifier works properly.

Fig. 13 shows the test results of the wireless isolated power supply system for two power supplies with no load and 1kΩ load conditions. Fig. 13(a) shows the voltage waveforms measured at the receiver side in no-load conditions. The resonance frequency of the received power supply voltage is 6.78 MHz and the output voltage of each power supply is 23V. In no-load conditions, the peak of antenna voltage is approximately equal to the output voltage. Fig. 13 (b) shows the voltage waveforms measured at the receiver side in load conditions. the output voltage of each power supply is 20V. These waveforms prove that the magnetic resonance wireless power transfer system works properly as an isolated power supply. Fig. 14 shows the start-up voltages of the output voltage of the power supply at the receiver. The output voltage of the power supply at the receiver is highly stable and has a 2-ms settling time after applying an enable signal to the

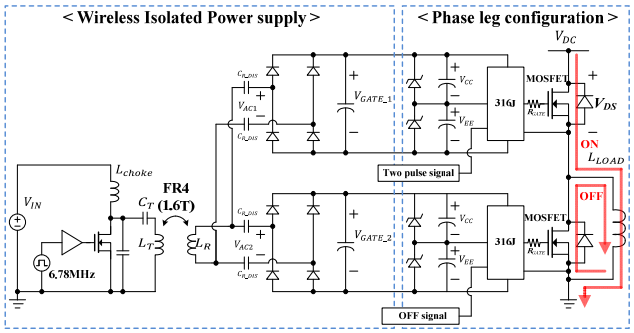

(a)

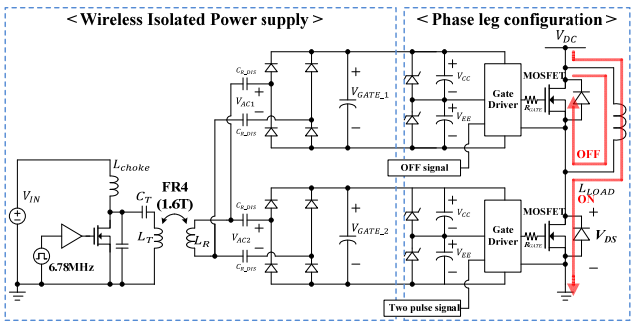

(b)

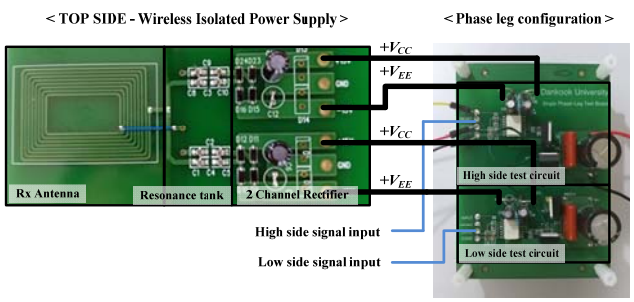

(c)

Fig. 15. Test board of a phase-leg configuration. (a) Low-side switch test circuit. (b) High-side switch test circuit. (c) Photo of test board.

transmitter. The efficiency of the power transfer system from Tx side input voltage to Rx side output with load is about 43.7% under the experimental conditions shown in Table I.

C. Gate Driver Test Board of Phase-Leg Configuration and Measurement Results

Fig. 15 shows the gate driver test circuit used to verify the isolation of each power supply when power is supplied to multiple gate drivers using a single Rx antenna. Fig. 15(a) shows the test circuit with high-side inductor load, and Fig. 15(b) shows the test circuit with low-side inductor load. The photo of gate driver test board for a single phase-leg condifuration is shown in Fig. 15(c). The power MOSFET and the gate-driver IC used in this circuit design are Infineon IPB65R660CFD and HCPL-316J, respectively [18] [19]. The test conditions of gate driver are shown in Table II.

Fig. 16 demonstrares the measured waveforms of V_{GATE_1} and V_{GATE_2} of each isolated power supply, with the I_{DRAIN} and

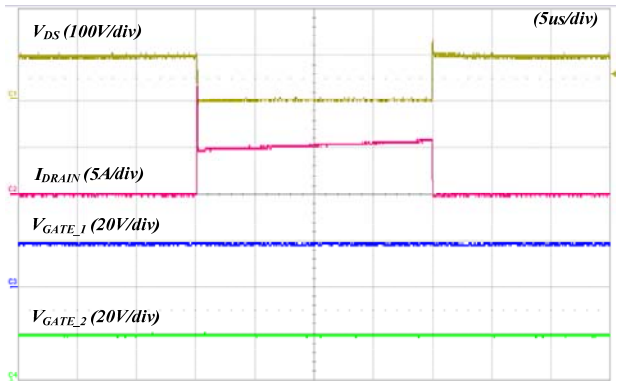

(a)

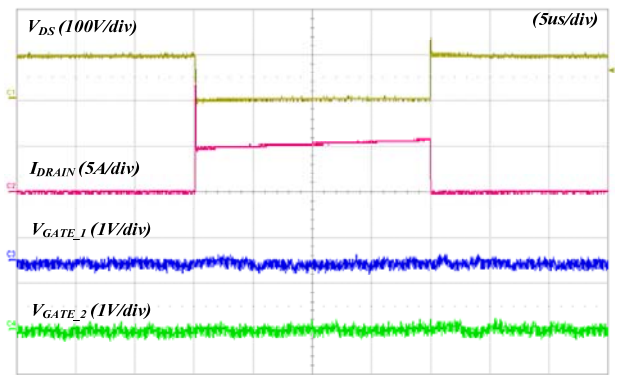

(b)

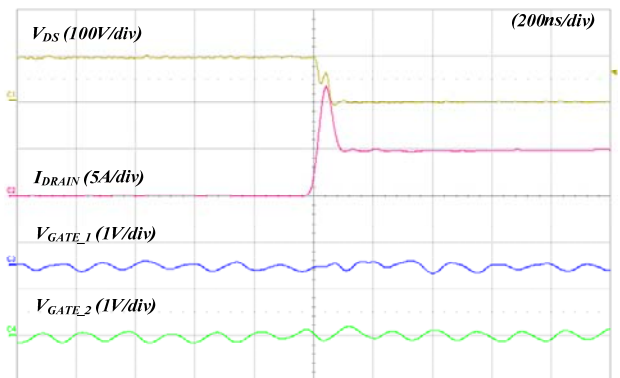

(c)

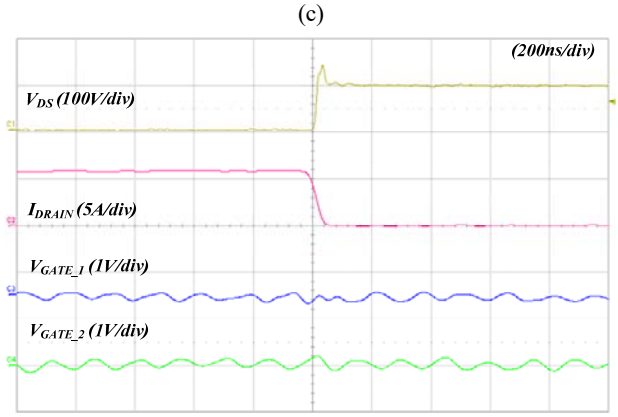

(d)

Fig. 16. Gate driver board test with high-side inductive load. (a) Waveforms of DC voltage. (b) Waveforms of AC ripple voltage. (c) Waveforms of AC ripple voltage at V_{DS} falling condition. (d) Waveforms of AC ripple voltage at V_{DS} rising condition.

TABLE II
GATE DRIVE TEST CONDITIONS

V_{DC}	100 V
I_{DRAIN}	5 A
t_{ON}	20 us
L_{LOAD}	2 mH
V_{CC}	15 V
V_{EE}	−5 V
R_{GATE}	10 Ω
C_{VCC}, C_{VEE}	10 uF

V_{DS} of low-side switch with a high-side inductive load. Fig. 16(a) shows the voltage waveforms of V_{GATE_1} and V_{GATE_2} with 20V/div voltage scale when the output voltage changes. Fig. 16(b) shows the expanded voltage waveforms of V_{GATE_1} and V_{GATE_2} to investigate voltage ripple in detail. Fig. 16(c) and Fig. 16(d) show the ripple voltage waveforms of V_{GATE_1} and V_{GATE_2} with an expanded time scale to focus on switching transient. From these test results, it is clear that the voltage ripple on V_{GATE_1} or V_{GATE_2} is very small during output voltage transition under high-side load condition.

Similary, Fig. 17 shows that the measured waveforms of V_{GATE_1} and V_{GATE_2} of each isolated power supply, but this time with the I_{DRAIN} and V_{DS} of high-side switch with a low-side inductive load. Fig. 17(a) shows the voltage waveforms of V_{GATE_1} and V_{GATE_2} with 20V/div voltage scale. Fig. 17(b) shows the expanded voltage waveforms of V_{GATE_1} and V_{GATE_2} to investigate the voltage ripple in detail. Fig. 17(c) and Fig. 17(d) show the ripple voltage waveforms of V_{GATE_1} and V_{GATE_2} with an expanded time scale to focus on switching transient. The measured voltage ripple with a low-side inductive load is about 1V, which is greater in amplitude than that of high-side inductive load. The voltage ripple difference between two condition can be explained as follows: The high-side switch always operates in saturation region while the low-side diode turns on during output voltage transition. This condition generates the low-impedance path between high-side and low-side power supply through gate-source of high-side switch and low-side diode. This low-impedance path causes a large voltage ripple during output voltage transition. Similary, under high-side load condition, the low-side switch operates in saturation region while the high-side diode turns on. However, in this case, the impedance path between high-side and low-side power supply becomes very high because the low-side switch plays the role of the current source during voltage transition. Therefore, the ripple voltage under high-side load condition is much less than that of low-side condition. From the test results, the maximum peak ripple voltage generated by $\frac{dV_{DS}}{dt}$ during high-side switching operation is 1V when $C_{R\_DIS} = 340$ pF and $C_{VOUT} = 10$ μF. This is less than 5% of the power supply voltage, 20V. It is apparent that the ripple voltage can be more effectively reduced if a higher value of C_{VOUT} is selected. From the test results, the distributed

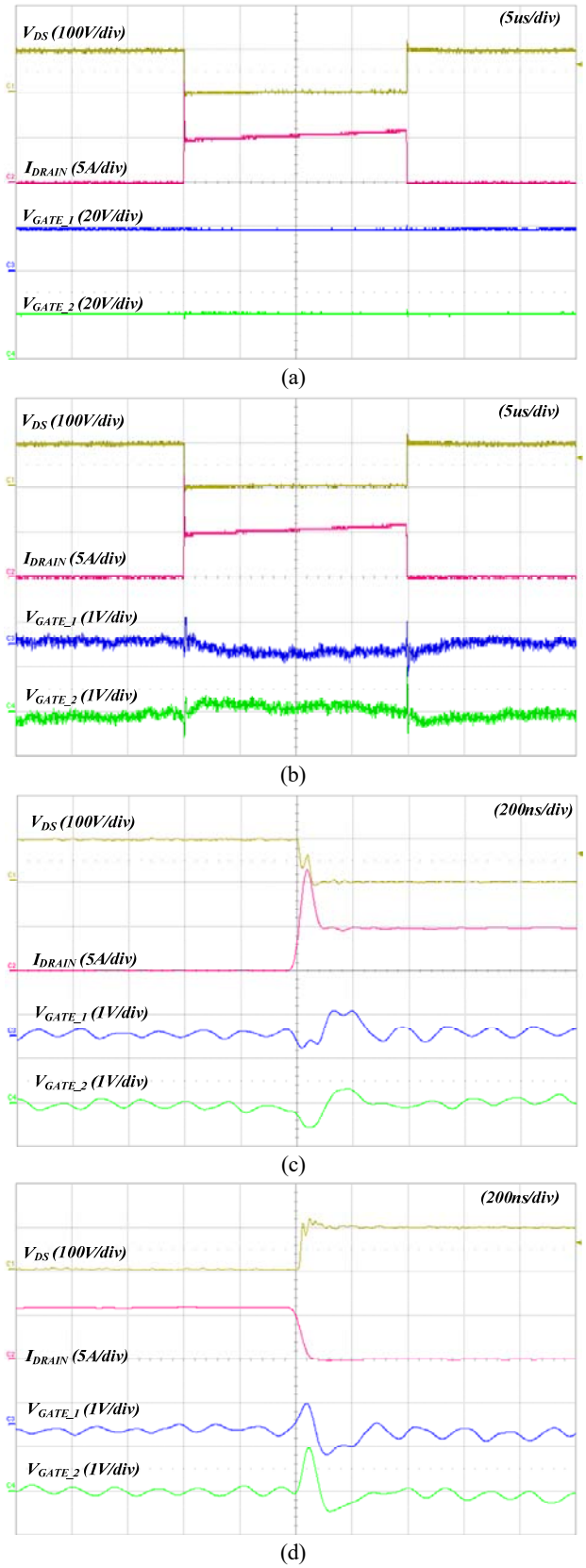

Fig. 17. Gate driver board test with low-side inductive load. (a) Waveforms of DC voltage. (b) Waveforms of AC ripple voltage. (c) Waveforms of AC ripple voltage at V_{DS} falling condition. (d) Waveforms of AC ripple voltage at V_{DS} rising condition.

TABLE III
PERFORMANCE COMPARISON

	This Work	Conventional Method[4]
Number of Tx ANTs	1	1
Number of Rx ANTs	1	6
Coupling	Resonance	Resonance
Frequency	6.78MHz	2.18MHz
Antenna Size	27.56 mm^2	44 mm^2
Galvanic Isolation	YES	YES

capacitors (C_{R_DIS}) block any interference from other power supplies and effectively isolate the power supply to drive the gate of each switch.

Table III shows the performance comparison between the conventional method and the proposed method. Unlike the conventional method, the proposed method uses only a single Rx antenna. Therefore, it offers a huge advantage in terms of reducing the cost and circuit area.

V. CONCLUSIONS

This paper describes an isolated power supply with a new structure, based on the magnetic resonance wireless power transfer method. The proposed structure is simple and provides isolated power to multiple gate drivers, using a single Rx antenna. By using a high resonance frequency of 6.78 MHz, a spiral PCB-type antenna could be implemented in a small area. When compared to conventional methods in an isolated power supply configuration, the proposed method demonstrates advantages such as reduction in cost and circuit area. The proposed method was verified by conducting PCB test board experiments, and it was verified that it could effectively isolate the power supplies to drive the gates of different switches. Therefore, this paper is expected to provide advantages in the implementation of various high voltage and high power applications.

ACKNOWLEDGMENT

The present research was conducted by the research fund of Dankook University in 2014.

REFERENCES

[1] HV floating MOS-gate drive ICs, in IR Application Note AN-978, International Rectifier Corp., El Segundo, CA.

[2] S. H. Park and T. M. Jahns, "A self-boost charge pump topology for a gate drive high-side power supply," *IEEE Trans. Power Electron.,* Vol. 20, No. 2, pp. 300-307, Mar. 2005.

[3] G. F. W. Khoo, D. R. H. Carter, and R. A. McMahon, "Analysis of a charge pump power supply with a floating voltage reference", *IEEE Trans. Circuits Syst.*, Vol. 47, No. 10, pp. 1494-1501, Oct. 2000.

[4] K. Kusaka, K. Orikawa, J. I. Itoh, K. Morita, and K. Hirao, "Isolation system with wireless power transfer for multiple gate driver supplies of a medium voltage inverter," in *Proc. IPEC*, pp. 191-198, 2014.

[5] K. Kusaka, K. Orikawa, J. I. Itoh, K. Morita, and K. Hirao, "Galvanic isolation system with wireless power transfer for multiple gate driver supplies of a medium-voltage inverter," *IEEJ J. Ind. Appl.*, Vol. 5, No. 3, pp. 206-214, May 2016.

[6] R. Steiner, P. K. Steimer, F. Krismer, and J. W. Kolar, "Contactless energy transmission for an isolated 100W gate driver supply of a medium voltage converter," *35th Annual Conference of IEEE Industrial Electronics,* pp. 302-307, 2009.

[7] C. Marxgut, J. Biela, J. W. Kolar, R. Steiner, and P. K. Steimer "DC-DC converter for gate power supplies with an optimal air transformer," in *Proc, APEC,* pp. 1865-1870, 2010.

[8] K. A. Grajski, R. Tseng, and C. Wheatley, "Loosely-coupled wireless power transfer: physics, circuits, standards," in *Proc. IMWS*, pp. 9-14, 2012.

[9] L. Sandrolini, U. Reggiani, G. Puccetti, and Y. Neau, "Equivalent circuit characterization of resonant magnetic coupling for wireless transmission of electrical energy," *Int. J. Circuit Theory Appl.*, Vol. 41, No. 7, pp. 753-771, Jul. 2013.

[10] S. Y. R. Hui, Y. X. Zhong, and C. K. Lee, "A critical review of recent progress in mid-range wireless power transfer." *IEEE Trans. Power Electron.,* Vol. 29, No. 9, pp. 4500-4511, Mar. 2013.

[11] X. Liu, W. M. Ng, C. K. Lee, and S. Y. Hui, "Optimal operation of contactless transformers with resonance in secondary circuits," in *Proc. APEC,* pp. 645-650, 2008.

[12] Y. Hasegawa, W. M. Ng, C. K. Lee, and S. Y. Hui, "Single-inductor-dual-output wireless power receiver with synchronous pseudo-random-sequence PWM switched rectifiers," in *Proc. A-SSCC,* pp. 261-264, 2013.

[13] T. Kawakiri, T. Moroto, and H. Ishikuro, "A low EMI SIDO wireless power transfer system with 10μsec response time," in *Proc. ESSCIRC,* pp. 253-256, 2015.

[14] R. Tseng, B. von Novak, S. Shevde, and K. A. Grajski, "Introduction to the alliance for wireless power loosely-coupled wireless power transfer system specification version 1.0," *IEEE Wireless Power Transfer,* pp. 79-83, 2013.

[15] M. Rooij, "Performance comparison for A4WP class-3 wireless power compliance between eGaN FET and MOSFET in a class E amplifier," *IEEE PCIM*, pp.1-8, 2015.

[16] M. K. Kazimierczuk, "Class E RF zero-voltage-switching RF power amplifier," in *RF Power Amplifiers*, Wiley, Chap. 5, 2008.

[17] N. O. Sokal and A. D. Sokal, "Class E a new class of high-efficiency tuned single-ended switching power amplifiers," *IEEE J. Solid-State Circuits*, Vol. 10, No. 3, pp. 168-176, Jun. 1975.

[18] Infineon, *IPB65R660CFD Datasheet*, www.infineon.com/dgdl/Infineon-IPX65R660CFD.pdf, 2011.

[19] Avago technologies, *HCPL-316J Datasheet*, www.broadcom.com/products/optocouplers/industrial-plastic/isolated-gate-drive-optocouplers/highly-integrated-smart-gate-drives/hcpl-316j.pdf, 2015.

Chang-Jong Yim was born in Suwon. He received the B.S., M.S., degrees in the Department of Electrical and Electronics Engineering from Dankook University, Yongin-si, Korea, in 2010, 2012 respectively. From 2012, he is working toward to obtain Ph.D. degree at Dankook University. His main research interest are power ICs, automotive power ICs, wireless power transfer, power converter circuits and power modules.

Shihong Park was born in Korea. He received the B.S. degree in electrical engineering from Yonsei University, Seoul, Korea, in 1988, and the M.S. and Ph.D. degrees from the University of Wisconsin, Madison, in 2003 and 2004, respectively. From 1988 to 1998, he was with Samsung Electronics, Buchen, Korea, as a Senior Power IC Design Engineer. In 2004, he was a Principal Research Engineer with Fairchild Semiconductor Korea, Buchen, Korea. In March 2005, he joined the School of Electronics and Electrical Engineering, Dankook University, Seoul. His main research interests are power ICs and devices for automotive applications, LED driver circuits, power converter circuits, active gate drive topology, and integrated power electronics modules (IPEMs).